Temperature dependence of the dielectric function and the interband critical-point parameters of GaP

Stefan Zollner,* Miquel Garriga,† Jens Kircher,‡ Josef Humlíček,§ and Manuel Cardona
Max-Planck-Institut für Festkörperforschung, Heisenbergstrasse 1, D-7000 Stuttgart 80, Germany

Georg Neuhold**
Institut für Technische Physik, Universität Erlangen, Erwin-Rommel-Strasse 1, D-8520 Erlangen, Germany
(Received 5 March 1993)

We have used spectroscopic ellipsometry to measure the dielectric function $\epsilon(\omega)$ of GaP from 10 to 640 K in the 1.6–5.6-eV photon-energy region. By performing a line-shape analysis of the observed structures, the interband critical-point (CP) parameters (strength, threshold energy, broadening, and excitonic phase angle) and their temperature dependence have been determined. Special emphasis is put on the E_0', $E_0'+\Delta_0'$, and E_2 CP's. We determine the spin-orbit splitting of Γ_{15}^c to be $\Delta_0'=160\pm10$ meV. The observed decrease in energy of the CP's (after correction for the effect of thermal expansion) and the corresponding increase in broadening with increasing temperature agree reasonably well with results of a calculation that takes into account the Debye-Waller and self-energy terms of the deformation-potential-type electron-phonon interaction. New local empirical pseudopotential form factors were fitted to the available band-structure data and used in the electron-phonon calculations.

I. INTRODUCTION

The band structure of a semiconductor is closely related to the dielectric function (DF) $\epsilon(\omega)$ of a material, which can be measured with optical techniques such as spectroscopic ellipsometry.[1] Conclusions about the electronic structure can be drawn from features in the spectra called critical points (CP's) which arise from Van Hove singularities in the joint density of states.[2,3] Such CP's have been studied in great detail using modulation techniques[4] such as electroreflectance.[3,5] Spectroscopic ellipsometry (SE) offers an alternative approach to the problem since the measured dielectric spectra can be differentiated numerically[6,7] yielding essentially the same features as electroreflectance.[3] Furthermore, SE has the advantage of being a nondestructive technique that does not perturb the sample in any way.

The DF can also be obtained from *ab initio* band-structure calculations[8] such as linear-muffin-tin-orbitals calculations,[9] or from empirical ones.[10] However, the agreement of the calculated optical constants (at least their absolute values) with experiment is not quite satisfactory, if the contribution of the excitonic Coulomb interaction is not taken properly into account.[11] Usually, the calculated $\epsilon_2(\omega)$ is found to be too small for the E_1 CP and too large for the E_2 peak. Such band-structure calculations are very useful, however, to assign CP's to transitions in certain areas of the Brillouin zone.[8,9] Meskini, Mattausch, and Hanke[12] have included local-field and excitonic many-body effects in a nonrelativistic calculation for GaP based on an empirical tight-binding Hamiltonian. This improves the agreement with experiment,[1] but some discrepancies still remain, in particular near the E_2 critical point.

Traditionally, it has been assumed that in the vicinity of a parabolic CP, the DF has the generic form[3]

$$\epsilon(\omega) = C - A\exp(i\phi)(\hbar\omega - E + i\Gamma)^n, \qquad (1)$$

which depends upon five parameters: the amplitude A, phase projection factor ϕ describing the type of CP (maximum, minimum, or saddle point) as well as excitonic effects,[11] threshold energy E, broadening parameter Γ, and exponent n (related to the dimensionality of the CP), see Refs. 3 and 13. For a three-dimensional (3D), 2D, 1D, and 0D (excitonic) CP, n has the values 1/2, 0 [logarithmic singularity, i.e., $\ln(\hbar\omega - E + i\Gamma)$], $-1/2$, and -1, respectively. Here, ω is the angular frequency of the incident light, and C is the nonresonant part of the DF due to other CP's. By calculating the derivative of the DF C will vanish. (See Ref. 14 for a critical review of this approach.)

In the past ten years, our group has been engaged in the systematic investigation of the dependence of the DF and interband CP's on temperature, concentration of donors and acceptors, and composition in mixed crystals using the technique of SE; see Ref. 15 and references therein. Parallel to this experimental work, calculations of the energy shifts[16,17] and broadenings[18] with temperature have been performed, taking into account the Debye-Waller[19,20] and self-energy[21] terms of the deformation-potential interaction.[15,22–25] This work gains additional technological importance by the fact that the same electron-phonon interactions that cause the temperature dependence of the CP parameters also determine the high-field transport properties of semiconductors.[18,26] In this paper we investigate ellipsometrically the temperature dependence of the optical constants (see Sec. II) and CP parameters (Sec. III) of undoped GaP for tempera-

tures from 10 to 640 K in the 1.6–5.6-eV photon-energy range and compare the temperature dependence of the CP energies and broadenings with theoretical predictions (Sec. IV).

II. EXPERIMENTAL SETUP AND RESULTS

The measurements were performed on samples cut from a nominally undoped ingot with (110) surface orientation. Similar results were obtained on a crystal with (100) orientation grown by isothermal vapor-phase epitaxy.[27] Before mounting the sample into the cryostat, a wet-chemical etching procedure[1,28] was performed in order to remove the oxide layer on the surface. Figure 1 shows the dielectric function thus obtained at room temperature (RT) in nitrogen atmosphere, corrected[29] for a 0.8-nm oxide layer[30] (solid line), in comparison with the data of Ref. 1 (•, △). The correction was necessary to achieve agreement of both spectra at the peak of ϵ_2 at 5.05 eV. After etching, the sample was quickly mounted inside a cryostat and measured at several temperatures between 10 and 640 K. Figure 1 also shows a spectrum inside the cryostat at RT, corrected for an oxide film of 0.8 nm on the surface (dotted line). The measurements were taken with an automatic spectral ellipsometer with rotating analyzer[1,31] described elsewhere.[32] The angle of incidence was always kept at 67.5° and the polarizer was set to 30° with respect to the plane of incidence.

In Figs. 2 and 3 we present the spectra obtained for the real and imaginary parts of the dielectric function of GaP for several temperatures after applying a correction for 0.8 nm of oxide on the GaP surface. In order to perform a line-shape analysis according to Eq. (1) and determine the CP parameters, we calculated numerically[6] the second derivative of the observed spectra, see Fig. 4 (○). The resulting curves are qualitatively similar to those observed in electroreflectance[33,34] and can be de-

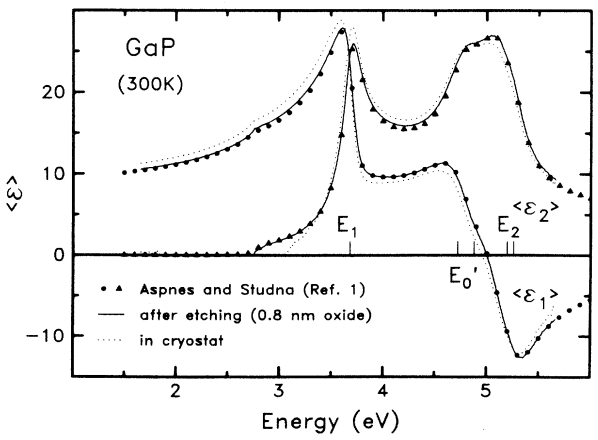

FIG. 1. Real (ϵ_1) and imaginary (ϵ_2) part of the dielectric function vs photon energy at 300 K, obtained directly after etching (solid line, corrected for 0.8 nm oxide) and after mounting inside the cryostat (dotted line) in comparison with the data of Ref. 1 (symbols).

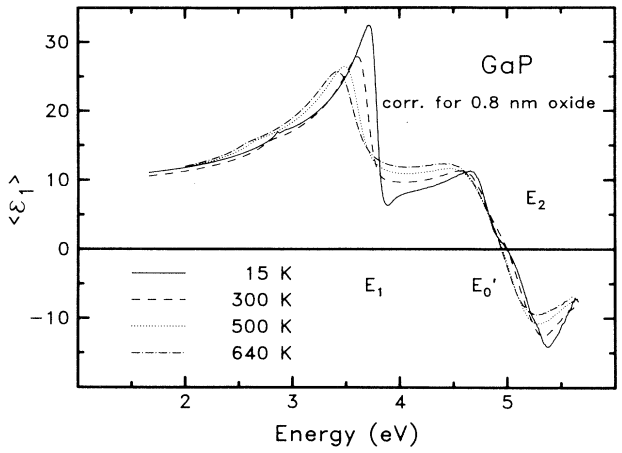

FIG. 2. Real part of the dielectric function (ϵ_1) at different temperatures, corrected for an oxide layer of 0.8 nm.

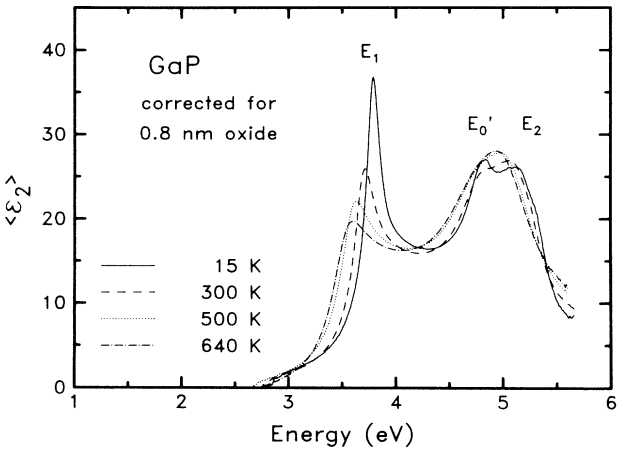

FIG. 3. As Fig. 2, but for ϵ_2.

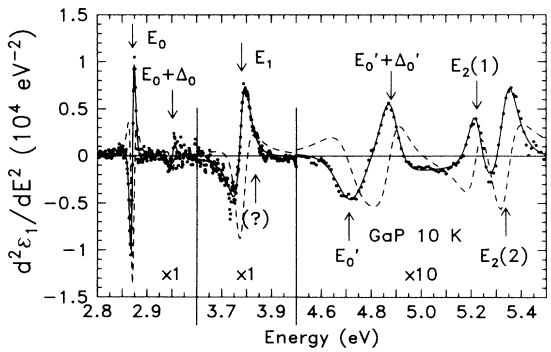

FIG. 4. Numerically calculated second derivative of ϵ_1 at 10 K in the vicinity of CP's (•), together with a line-shape fit according to Eq. (1) (solid line) with the parameters given in Table I. The dashed line shows the imaginary part of the fit. The readings on the vertical scale have to be divided by the factors given below the structures. The arrows indicate the energy positions of the CP's. Note the change in the scale on the horizontal axis for the E_0 and $E_0 + \Delta_0$ CP (between 2.8 and 3.0 eV).

TABLE I. Parameters of the critical points (CP's) of GaP at 10 K determined by a complete line-shape analysis. For a 3D (0D) CP the amplitudes A have the dimension $\mathrm{eV}^{-1/2}$ (eV), they are dimensionless for a 2D CP. The numbers in parentheses give the 95% confidence limits. The values for $E_1 + \Delta_1$ are a rough estimate compatible with our experimental data.

GaP	E (eV)	Γ (meV)	ϕ (deg)	A	Line shape
E_0	2.870 (1)	4 (1)	18 (16)	11 (2)	3D
E_0	2.870 (1)	9 (2)	0 (5)	0.004 (1)	0D
$E_0 + \Delta_0$	2.949 (1)	8 (2)	35 (2)	3.7 (3)	3D
$E_0 + \Delta_0$	2.950 (1)	15 (2)	−17 (13)	0.002 (1)	0D
E_1	3.780 (2)	40 (2)	120 (9)	15 (2)	2D
E_1	3.780 (3)	57 (3)	29 (9)	0.7 (2)	0D
$E_1 + \Delta_1$	3.835 (?)	60 (?)	120 (?)	8 (?)	2D
E_0'	4.715 (9)	98 (9)	330 (9)	41 (9)	3D
$E_0' + \Delta_0'$	4.879 (8)	63 (6)	173 (9)	24 (5)	3D
$E_2(1)$	5.227 (7)	63 (7)	181 (16)	16 (4)	3D
$E_2(2)$	5.340 (5)	44 (9)	123 (14)	39 (9)	3D

scribed well with the analytical line shapes (solid lines) of Eq. (1) with the parameters given in Table I.

III. DISCUSSION

GaP is an indirect semiconductor, similar to AlAs or AlSb. Its band structure, as calculated by Chelikowsky and Cohen[35] using the empirical nonlocal pseudopotential technique without spin-orbit (SO) splitting, is shown in Fig. 5. Recent angle-resolved photoemission measurements[36,37] in several symmetry directions have shown that these calculations yield valence-band (VB) energies that are accurate up to at least 0.3 eV. The lower conduction-band (CB) energies are accurate also (since the energy gaps were adjusted by varying the pseudopotential form factors), but substantial differences[37] were found at energies between 7 and 20 eV (not shown in Fig. 5). Similar band structures have been obtained with a full-zone 15×15 $\mathbf{k}\cdot\mathbf{p}$ calculation[38] (with SO splitting) and a combined pseudopotential–tight-binding approach.[39] *Ab initio* band-structure calculations, mainly with the nonlocal pseudopotential method and based on the local-density approximation, have also been performed.[40–45]

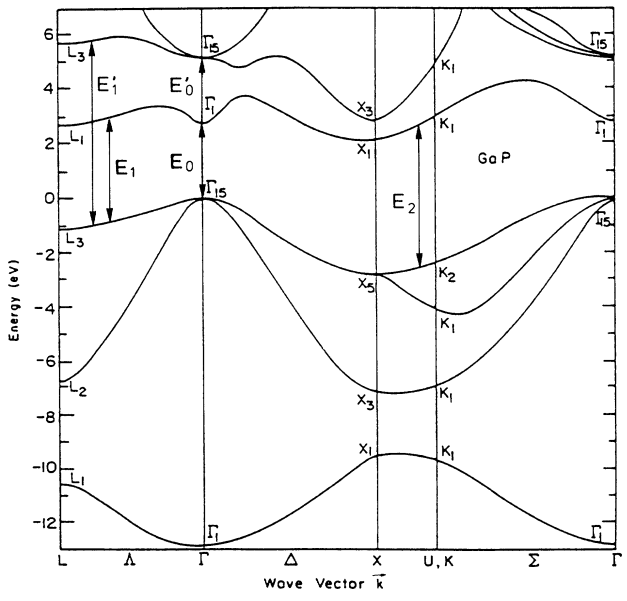

FIG. 5. Calculated band structure of GaP (without spin-orbit interaction), taken from Ref. 35. Several interband critical-point (CP) transitions are indicated. The assignment of the E_2 CP is tentative.

Several interband transitions related to CP's at different parts of the Brillouin zone are indicated and will be discussed below. Such CP's have been studied extensively[35,46] using absorption,[47–58] electroabsorption,[59,60] photoemission,[36,37,61] spectroscopic ellipsometry,[11] photoconductivity,[62] wavelength-modulated photoconductivity,[63] reflectance,[64–71] and several reflectance-modulation techniques, such as energy derivative reflectance,[72] magnetoreflectance,[73] thermoreflectance,[74,75] electroreflectance,[33,34,76,77] piezoreflectance,[78] and wavelength-modulated reflectance.[79,80] We give the results of some of these measurements and those of band-structure calculations[81–85] in Table II. The temperature dependence of various CP's, especially the indirect and lowest direct gaps, has also been measured.[86] In Table III we list the linear temperature coefficients determined by various groups. In order to understand the electron-phonon interactions that cause the temperature shifts, it is necessary to go beyond this linear dependence.[50,80]

A. Critical points

The lowest indirect interband transition, with an energy of 2.350 eV at 0 K, see Ref. 46, takes place from the VB maximum at Γ to the absolute CB minimum near X (X_1). A second indirect gap to the CB minimum at L occurs at 2.637 eV (see Refs. 46 and 60). The latter transition is almost degenerate with a third indirect transition to the second lowest CB at X with X_3 symmetry[44] (2.69 eV). These indirect transitions cannot be observed in ellipsometry since they are very weak. For the ellipsometer, the crystal is essentially transparent ($\epsilon_2 < 1$,

TABLE II. Experimental and theoretical CP energies (in eV) for GaP at several temperatures T (in K). We used the calculated band energies at the X point to obtain the theoretical E_2 energies.

T	E_0	$E_0+\Delta_0$	E_1	$E_1+\Delta_1$	E_0'	$E_0'+\Delta_0'$	$E_2(1)$	$E_2(2)$	$E_2+\delta$
				Experiment					
2[a]	2.869 (1)	2.949 (1)	3.785 (5)	3.835 (5)	4.77 (1)	4.85 (1)	5.21 (1)	5.36 (1)	5.50 (2)
10[b]	2.870 (1)	2.949 (1)	3.780 (2)	3.835 (?)	4.727 (9)	4.881 (8)	5.228 (7)	5.340 (9)	
80[c]	2.85 (5)	2.93 (5)	3.91 (10)		4.87 (10)		5.5 (1)		
80[d]			3.76		4.82	4.88			
80[e]	2.82		3.83	3.91	4.6				
110[f]							5.2	5.3	6.44
300[a]	2.780 (2)	2.860 (2)	3.693 (2)		4.77 (1)		5.12 (1)	5.34 (1)	
300[b]									
300[g]	2.8		3.7		4.8		5.3		
300[h]	2.74	2.84	3.66,3.80		4.78	4.83	5.27		5.74
300[i]	2.750	2.845	3.662,3.803		4.751	4.81	5.275		5.739
300[j]			3.71						
300[k]							5.37		5.80
300[l]	2.725	2.775	3.650,3.785		4.68		5.2		
300[m]	2.757								
0[m]	2.866	2.946 (3)							
25[n]	2.873 (1)	2.954 (1)							
25[o]	2.884 (1)	2.962 (2)							
300[p]	2.76 (1)								
77[q]	2.888 (4)								
89[r]	2.865	2.944							
300[s]			3.7				5.3		
300[t]			3.71						
290[u]	2.8	2.9	3.69	3.78	4.68	4.80	5.3		
300[v]			3.7				5.3		
300[w]	2.75							δ=0.29	
300[x]	2.78	2.88	3.75	3.85					
300[y]			3.7						
80[z]							δ=0.357 (2)		
300[aa]							δ=0.340		
300[bb]							δ=0.35		
295[cc]							δ=0.29 (1)		
295[dd]							δ=0.355 (3)		
				Theory					
0[ee]		Δ_0=0.09	Δ_1=0.06		Δ_0'=0.17				
0[ff]		2.888	3.594		4.892		4.739		5.107
0[gg]		2.05	3.52		4.26		4.51	4.64	4.81
0[hh]		1.89	2.74		3.94		4.14		4.35
0[ii]		2.93	3.83		4.42		4.77		5.19
0[jj]		2.83	3.51		4.73		4.52		
0[kk]		2.09			2.94		4.30		
0[ll]		3.61	4.73		4.73		6.07		
0[mm]		2.272							
0[nn]		1.56	2.57				4.27		4.39
0[oo]		2.82	3.58		5.17			δ=0.31	
0[pp]		1.40	2.97		4.07		4.01		
0[qq]		2.7	3.6		5.3		4.6		5.0
0[rr]		2.79	3.70		4.7		5.3		
0[ss]		2.88	3.89		5.24		4.89		5.44
0[tt]		2.84	3.67		4.75		5.28		
0[uu]	2.88	2.97	5.09	5.16	5.06	5.20	9.22	9.24	9.69
0[vv]		3.11	3.38		4.89		4.41		4.77

[a]Energy-derivative reflectance, Ref. 72.
[b]Spectroscopic ellipsometry (this work).
[c]Electroreflectance, Ref. 34.
[d]Wavelength modulation, Ref. 79.
[e]Differential magnetoreflection, Ref. 73.
[f]Thermoreflectance, Ref. 75.
[g]Thermoreflectance, Ref. 74.
[h]Electroreflectance, Ref. 33.
[i]Electroreflectance, Ref. 76.
[j]Reflectance, Ref. 64.
[k]Reflectance, Ref. 70.
[l]Piezoreflectance, Ref. 78.
[m]Wavelength modulation, Ref. 80.
[n]Absorption, Ref. 48.
[o]Absorption, Ref. 49.
[p]Absorption, Ref. 52.
[q]Photoconductivity, Ref. 62.
[r]Wavelength-modulated photoresponse, Ref. 63.
[s]Reflection, Ref. 65.
[t]Reflection, Ref. 67.

TABLE II. (*Continued*).

[u]Reflection, Ref. 68.
[v]Reflection, Ref. 69.
[w]Electroabsorption, Ref. 59.
[x]Electroreflectance, Ref. 77.
[y]Spectroscopic ellipsometry, Ref. 11.
[z]Absorption, Ref. 53.
[aa]Absorption, Ref. 54.
[bb]Absorption, Ref. 55.
[cc]Absorption, Ref. 58.
[dd]Absorption, Ref. 57.
[ee]Orthogonalized-plane-wave model (relativistic, including exchange-correlation effects), Ref. 93.
[ff]Empirical local pseudopotential method, this work.
[gg]Self-consistent linear combination of Gaussian orbitals (nonrelativistic, uncorrected LDA), Ref. 8.
[hh]*Ab initio* pseudopotential calculation (nonrelativistic, nonlocal, uncorrected LDA), Ref. 40.
[ii]*Ab initio* pseudopotential calculation (nonrelativistic, local, corrected LDA), Ref. 40.
[jj]*Ab initio* pseudopotential calculation (nonrelativistic, nonlocal, corrected LDA), Ref. 41.
[kk]*Ab initio* pseudopotential calculation (nonrelativistic, nonlocal, uncorrected LDA), Ref. 42.
[ll]*Ab initio* pseudopotential calculation (nonrelativistic, nonlocal, uncorrected LDA), Ref. 43.
[mm]Linear-muffin-tin-orbitals method (relativistic, uncorrected LDA), Ref. 44.
[nn]Nonlocal empirical pseudopotential method, Ref. 83.
[oo]*Ab initio* pseudopotential calculation (nonrelativistic, local, uncorrected LDA), Ref. 45.
[pp]Empirical local pseudopotential method, Ref. 81.
[qq]Empirical local pseudopotential method, Ref. 82.
[rr]Empirical nonlocal pseudopotential method (without spin-orbit coupling), Ref. 35.
[ss]Model pseudopotential calculation, Ref. 84.
[tt]Tight-binding calculation with estimate of spin-orbit splittings, Ref. 85.
[uu]Tight-binding calculation (Gaussian orbitals), Ref. 39.

TABLE III. Linear temperature coefficients of CP energies for GaP (in 10^{-4} eV/K).

$-\frac{dE_i}{dT}$	$-\frac{dE_0}{dT}$	$-\frac{dE_1}{dT}$	$-\frac{dE_0'}{dT}$	$-\frac{dE_2}{dT}$	Source
		Experiment			
		Between 100 and 300 K			
3.57					Ref. 50
2.36 (1)	5.2 (1)				Ref. 48
4.2					Ref. 59
	4.7				Ref. 62
5.2	4.6				Ref. 66
5					Ref. 69
		3.7 (9)			Ref. 68
	5.1				Ref. 80
		2.8 (1.0)	3.3 (1.0)	4.2 (1.4)	Ref. 71
		2.6 (6)			Ref. 64
	5.0 (2)	4.3 (1)	3.1 (6)	2.6 (6)	this work
		Between 300 and 500 K			
5.0 (3)	6.5 (6)				Refs. 47, 59
	6.2				Ref. 80
		5.5 (2)	3.7 (8)	3.5 (8)	this work
		Theory (at 300 K)			
	5.1				DW+TE+SE[a]
4.3	4.5	2.8		2.5	DW+TE[b]
4.6	6.8	5.6	4.3		DW+TE+SE[c]
5.0	5.5	4.2	3.3		DW only[c]
−0.3	1.2	0.5	0.1		TE only[c]
−0.1	0.1	0.9	0.9		SE only[c]

[a]Reference 106.
[b]Reference 105.
[c]This work.

$\alpha < 30\times10^3$ cm^{-1}) below the direct gap E_0 at 2.87 eV (at 0 K, see Table I). In this energy range measurements with a rotating-analyzer ellipsometer (RAE) without compensator are not very sensitive to ϵ_2 because of the RAE artifact.[1] (An RAE measures $\cos\Delta$ and therefore is not very accurate if $\Delta \sim 0$.)

Figure 6 shows the real part of the DF between 2.7 and 3.0 eV, in the vicinity of the direct gap at 10 and 300 K. In the low-temperature data, one peak (E_0=2.87 eV) and a shoulder ($E_0 + \Delta_0$=2.949 eV) can be seen. Both are caused by direct optical transitions from the spin-split top of the VB at Γ to the (relative) CB minimum. The energies of both transitions at 10 K, determined from a line-shape analysis (see Fig. 4), along with the other CP parameters can be found in Table I. It can be seen that the CP's broaden and shift to lower energies with increasing temperature. At higher temperatures the value of Δ_0=80 meV was fixed in the fitting procedure. With the numerical derivative approach, we could obtain the energies of E_0 up to 360 K. Previous data existed only at room temperature and below.[80] This doublet can be fitted with an excitonic or 3D line shape, see Table I.

We find the temperature dependence of ϵ_1 below the gap to be $d\epsilon_1/dT = +2\times10^{-3}$ at 2.7 eV, in agreement with the temperature dependence of the refractive index $dn/dT = +2\times10^{-4}$ at 2.2 eV determined in Ref. 69 using the prism method. From this we calculate a reflectivity change between 10 and 300 K of only 0.7% (compare Ref. 87), three times smaller than determined with a reflectivity measurement (see Fig. 3 in Ref. 72). The absolute values of the optical constants in this energy range are essentially in agreement with Refs. 1, 69, and 72, but larger than those calculated from the model in Ref. 80, Fig. 6. The dispersion of the refractive index below the gap can be described with analytical models based on a Sellmaier-type equation (with two[69] or three[88] Lorentzian oscillators) or an interband CP model[89] as described elsewhere.[90] Above the direct gap, analytical models are less accurate,[91] except for the recent work of Kim *et al.*[14]

Above 3 eV the absorption rises sharply to a maximum near 3.6 eV, see Fig. 1. The origin of this very strong peak

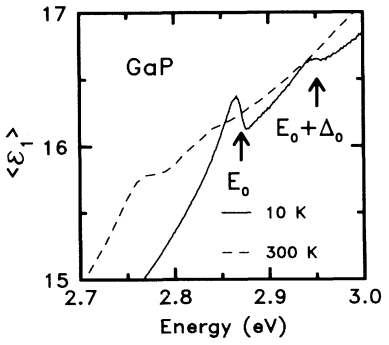

FIG. 6. ϵ_1 in the vicinity of the direct gap at 10 K (solid line) and 300 K (dashed line). The arrows show the positions of the E_0 and $E_0+\Delta_0$ CP's at 10 K. At 300 K, the CP's have moved to lower energies and the broadenings have increased. (Compare the absorption data in Fig. 1 of Ref. 49.)

(labeled E_1 with an energy of 3.78 eV at 10 K, see Table I) that could be observed up to 670 K has been somewhat controversial.[67,78] Band-structure calculations[8,35] assign it to transitions along the Λ directions and in the ΓKL plane, just as in most other semiconductors.[9] Two experimental observations confirm this assignment: (1) Temperature and pressure shifts of this peak are similar to those of the E_1 peak of silicon[92] at 3.4 eV, but noticeably smaller than for the corresponding E_1 transitions in other materials.[67] (2) In $GaAs_{1-x}P_x$ alloys,[71,76] this peak clearly can be followed to the E_1 transitions in GaAs. However, there is a clear break in the slope of the energy versus composition plot (see Fig. 13 in Ref. 76 and Fig. 1 in Ref. 71). Therefore, it has been suggested that the E_1 peaks in GaP and GaAs both are due to transitions along [111], but have different origins all the same.[71] This has not been confirmed with band-structure calculations.[8,35]

It can be seen from Fig. 4 that one CP is sufficient to describe the observed shape of the derivative spectrum in the E_1 range. Both 2D and 0D (excitonic) line shapes can be used to determine the CP parameters, see Table I. (In the older literature[76] it has sometimes been assumed that the E_1 CP is caused by two transitions along [111], but the line-shape analysis due to Cardona[4] and Aspnes[3] makes this viewpoint obsolete. We note that Takizawa, Fukutani, and Kawabara[78] concluded from piezoreflectance studies that the E_1 peak in GaP was caused by two singularities located along the [001] and [110] directions.) From the SO splitting Δ_0=79 meV of the VB top and the two-thirds rule[85] we expect a SO splitting $\Delta_1 \sim 50$ meV in the topmost VB along Λ. One therefore expects an additional CP $E_1+\Delta_1$ at about 3.83 eV, marked by a question mark in Fig. 4. Stokowski and Sell[72] indeed find a small satellite of E_1 in the logarithmic derivative of the reflectivity at 2 K near 3.9 eV, which we can barely reproduce in the derivative of the reflectance calculated from our ellipsometric data. The structure is too weak, however, to perform a line-shape analysis. The CP parameters given for $E_1+\Delta_1$ in Table I are merely an intelligent guess compatible with our data based on experience with similar materials.[15]

It is striking that the broadening parameter Γ of the E_1 transition is rather large when compared to other materials[18] although the electron-phonon interaction (source of the broadening) is expected to be weaker.[18,26] We note that Δ_1 is equal to typical optical phonon energies in GaP, and therefore suggest a very effective interband transfer of photoexcited holes from the top valence band ("heavy hole" with $\Lambda_{4,5}$ symmetry) to the second-highest VB ("light hole," Λ_6 symmetry) increasing the broadening of E_1. This mechanism is not possible in any other material except silicon (where it is difficult to observe because of the overlap of the E_1 and E_0' structures[92]) and is not included in the calculations of Ref. 18. From this we conclude that the broadening of the E_1 transition should be larger than that of the $E_1+\Delta_1$ CP for moderate temperatures (below the Debye temperature), since a hole in the $\Lambda_{4,5}$ VB can emit a phonon and scatter to Λ_6, but not vice versa. (The fact that the E_1 and $E_1+\Delta_1$ CP's cannot be resolved in the experiment may also increase the observed broadenings,

but this cannot account for all of the effect.)

We now proceed to discuss the E_0' and $E_0'+\Delta_0'$ CP's: It may seem that the line shape of $d^2\epsilon_1/dE^2$ between 4.5 and 5.0 eV is similar to that of the E_1 CP (a minimum followed by a maximum), but a quantitative analysis (see Fig. 4) shows that the observed shape can only be described by two CP's with different phase angles, which we label E_0' and $E_0'+\Delta_0'$, see Table I. The energy difference between these two CP's is Δ_0'=0.16(1) eV, very close to a tight-binding estimate[85] for the splitting Δ_0'=0.14 eV of the p-antibonding CB at Γ. An older, but more sophisticated calculation[93] using a relativistic orthogonalized plane-wave model including exchange-correlation effects to solve the Dirac equation yields Δ_0'=0.17 eV. (The Γ_{15} VB mainly has phosphorus character, the corresponding CB mainly gallium; therefore Δ_0' should be expected to be larger than Δ_0, see Ref. 85.)

In analogy with measurements on GaSb (Ref. 15) and band-structure calculations[9] for GaAs, we assign E_0' to transitions from the Γ_8 VB to the Γ_7 CB, and $E_0'+\Delta_0'$ to transitions to the Γ_8 CB. The transition $E_0'+\Delta_0+\Delta_0'$ ($\Gamma_7^v \rightarrow \Gamma_8^c$) should occur at 4.96 eV (10 K), but was not observed. $E_0'+\Delta_0$ ($\Gamma_7^v \rightarrow \Gamma_7^c$) is forbidden by group theory in the dipole approximation. In analogy to other materials like GaSb (Ref. 15) we also expect a structure labeled $E_0'(\Delta)$ very close to E_0' (caused by transitions to the pseudocrossing of the two lowest CB's along Δ, see Ref. 35), but no additional structure was found in this energy range.

Above 5 eV we observe two CP's that are part of the multiplet labeled E_2. The stronger one of these is probably caused by transitions from a plateau in the joint density of states in the Γ-X-U-L plane near the point P=(0.75,0.25,0.25), in units of $2\pi/a$; see Ref. 9. We therefore tentatively write $E_2(P)$=5.34 eV. The weaker structure is probably[35] due to transitions along the Δ direction near the Brillouin-zone boundary and labeled $E_2(\Delta)$=5.23 eV. We also expect four CP's at the X point (between 5.3 and 5.7 eV) and an $E_2+\delta$ transition inside the Brillouin zone to the second-lowest conduction band (about 0.4 eV higher than E_2), but these transitions either occur at energies higher than 5.5 eV (and are therefore outside of the spectral range of our ellipsometer) or are hidden by the stronger features.

Figure 4 shows that there is a considerable overlap between the various E_0' and E_2 structures. Therefore, all four CP's between 4.5 and 5.5 eV were fitted simultaneously with 3D singularities [see Eq. (1)], requiring sixteen free parameters. The 95% confidence limits given in Table I prove that in spite of the large number of parameters the Hessian of the system of nonlinear equations is well conditioned, at least at 10 K. Ten different spectra, taken with three different samples, gave parameters in agreement with each other. At temperatures above 300 K, however, the broadenings of the CP's increase, and it becomes very difficult to find exact CP parameters.

B. Temperature dependence of CP parameters

In a simple Einstein model for the crystal (in which all phonons have the same energy Ω) with Einstein temperature $\Theta=\Omega/k_B$, the electron-phonon contribution to the temperature shifts of the band gaps can be written as[22,32]

$$E(T) = E_B - a_B(2N_\Omega+1) = E_B - a_B\left[1+\frac{2}{\exp(\Theta/T)-1}\right], \quad (2)$$

where E is the observed band gap as a function of temperature T, E_B the unrenormalized energy of creating an electron-hole pair, a_B the strength of the electron-phonon coupling, and N_Ω the Bose-Einstein occupation factor. (A microscopic theory for the temperature shifts, including details of the electronic and lattice properties of GaP, will be given in Sec. IV.) This equation has the same functional form as the Manoogian-Leclerc relation,[94]

$$E(T) = E_0 - A[\coth(T_0/T)-1], \quad (3)$$

if we set $E_0 = E_B - a_B$, $A = a_B$, and $2T_0 = \Theta$. The "new three-parameter fit" suggested recently[95] is not new at all, but simply a new reiteration of the same Einstein model. For temperatures higher than the Einstein temperature, Eq. (2) is approximately equal[96] to the Varshni expression[97]

$$E(T) = E_0 - \frac{\alpha T^2}{T+\beta}, \quad (4)$$

where $\alpha = 2a_B/\Theta$ and $\beta = \Theta/2$.

In Fig. 7 we show the temperature dependence of the E_0 (•) and E_1 (□) CP energies determined from the fitting procedure. The solid lines show a fit to the data with Eq. (2) leading to the parameters in Table IV. A fit with Eq. (4) was also performed (not shown in the figure). The dotted lines (shifted to agree with the ex-

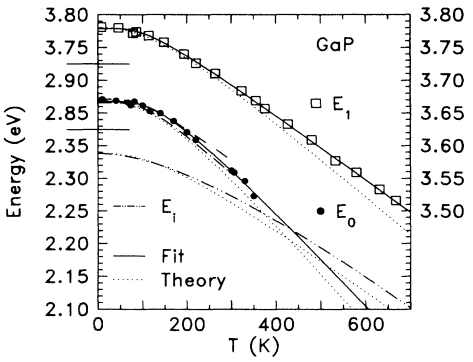

FIG. 7. Temperature dependence of the interband CP energies (for E_0, E_1, and the indirect gap E_i) of GaP as obtained from a line-shape fit to ellipsometric data (•,□). The solid lines represent the best fits to the data with Eq. (2), the dotted lines give the results of a parameter-free calculation as outlined in Sec. IV. Data from the literature are also given: The dashed and dashed-dotted lines show the results obtained for E_0 in Refs. 48 and 80, respectively, the dashed–double-dotted line shows the temperature dependence of the indirect gap from Ref. 50.

TABLE IV. Parameters E_B, Θ, and a_B obtained by fitting the CP energies vs temperature to Eq. (2), and values of $E(0)$, α, and β obtained by fitting with Eq. (4). The numbers in parentheses indicate the 95% error margins; (f) indicates that the parameter was fixed during the fit. Values for E_i and E_0 taken from the literature are also shown.

	E_B (eV)	a_B (eV)	Θ (K)	$E(0)$ (eV)	α (10^{-4} eV K^{-1})	β (K)	Line shape
E_0	3.02 (4)	0.15 (4)	400 (67)	2.877 (3)	9.6 (4)	460 (f)	exc.
E_1	3.858 (7)	0.079 (9)	290 (26)	3.785 (3)	6.1 (4)	240 (53)	exc.
E_0'	4.76 (1)	0.052 (7)	290 (f)				3D
$E_0' + \Delta_0'$	4.92 (2)	0.026 (9)	290 (f)				3D
$E_2(1)$	5.27 (2)	0.051 (7)	290 (f)				3D
$E_2(2)$	5.42 (3)	0.067 (10)	290 (f)				3D
E_i				2.338	6.2	460	Ref. 50
E_0	2.974	0.1081	328				Ref. 80
E_0	2.947	0.0756	288				Refs. 48, 80

perimental data at 0 K) show the results of a parameter-free calculation described in Sec. IV. The data for the temperature-dependent E_0 energies determined in Refs. 48 and 80 are given by the dashed and dashed-dotted lines, respectively. For comparison, the energies of the lowest indirect gap E_i (from Ref. 50) are also given in Fig. 7 (dashed–double-dotted line). The linear temperature coefficients calculated from these data can be found in Table III.

By the same token, Fig. 8 shows the energies of the E_0', $E_0' + \Delta_0'$, $E_2(1)$, and $E_2(2)$ CP's as a function of temperature. As stated above, these data are rather inaccurate above 300 K. For example, Δ_0' should not depend on temperature since it is of atomic origin. Therefore, the experimental temperature coefficients of the E_0' and $E_0' + \Delta_0'$ CP energies should be taken as the upper and lower limits for dE_0'/dT. The difference between $dE_2(1)/dT$ and $dE_2(2)/dT$ also is not significant.

Our line-shape analysis allows not only the CP energies to be determined, but also the other CP parameters, i.e., the broadening Γ, phase angle ϕ, and amplitude A, see Eq. (1). The broadenings of CP's observed in semiconductors can generally have several sources, both intrinsic and extrinsic. The latter include improper preparation of the sample surface (causing, e.g., microscopic roughness or amorphization), intrinsic surface effects, lateral gradients of composition or oxide layer thickness, overlap of several critical points, smoothing of the curves when calculating the numerical derivatives,[7] spectral resolution of the monochromator, etc. We have tried very carefully to minimize the artifacts. The intrinsic source which we study here is the following: After the creation of an electron-hole pair, one of the carriers may scatter to a different point in **k** space thereby causing a lifetime broadening. In a binary compound semiconductor with moderate doping the main mechanism is the deformation-potential electron-phonon interaction[23] (we will give the results of a microscopic theory in Sec. IV), except for the E_0 gap in a direct material where the Fröhlich interaction is also important.[98,99] In an alloy[100] or a heavily doped semiconductor,[101] the carriers can also be scattered by impurities, but this is not relevant here.

With the Einstein model, the broadenings as a function of temperature can be described by the expression,[32,99] similar to Eq. (2),

$$\Gamma(T) = \Gamma_0 (2N_\Omega + 1) + \Gamma_1, \tag{5}$$

where the second term allows for temperature-independent broadenings (such as intrinsic surface effects) and the first one is due to electron-phonon interactions.

The broadenings Γ of the E_0 (•) and $E_0 + \Delta_0$ (○) gaps, fitted with excitonic line shapes, are shown in Fig. 9(a). The solid lines show a fit to the data with Eq. (5) (with parameters given in Table V). Our data for $\Gamma(E_0)$ at 10 K are consistent with those of Sell and Lawaetz[49] who found $\Gamma(E_0)$=6 meV from transmission measurements. However, we find $\Gamma(E_0)$ and $\Gamma(E_0 + \Delta_0)$ to be essentially the same, whereas Ref. 49 claims that $\Gamma(E_0 + \Delta_0) = 2\Gamma(E_0)$. With the arguments presented in Ref. 7, it should seem

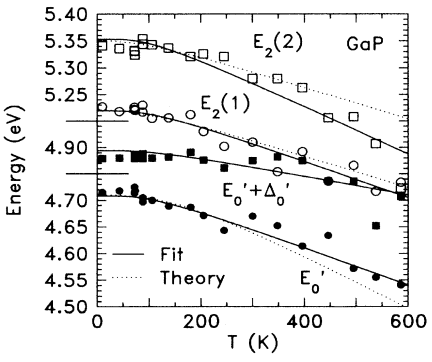

FIG. 8. As Fig. 7, but for the E_0' and E_2 CP's.

TABLE V. Parameters Γ_0, Θ, and Γ_1 obtained by fitting the CP broadenings vs temperature to Eq. (5). The numbers in parentheses indicate the 95% error margins; (f) indicates that the parameter was fixed during the fit.

CP	Γ_0 (meV)	Θ (K)	Γ_1 (meV)	Line shape
E_0	10 (3)	220 (170)	0 (f)	0D
E_0	4 (1)	240 (900)	0 (f)	3D
$E_0 + \Delta_0$	11 (1)	123 (53)	0 (f)	0D
E_1	68 (3)	480 (30)	0 (f)	0D
E_1	45 (5)	500 (50)	0 (f)	2D
E_0'	87 (20)	301 (2)	0 (f)	3D
$E_0' + \Delta_0'$	66 (11)	680 (30)	0 (f)	3D
$E_2(1)$	46 (7)	510 (30)	0 (f)	3D
$E_2(2)$	62 (9)	600 (25)	0 (f)	3D

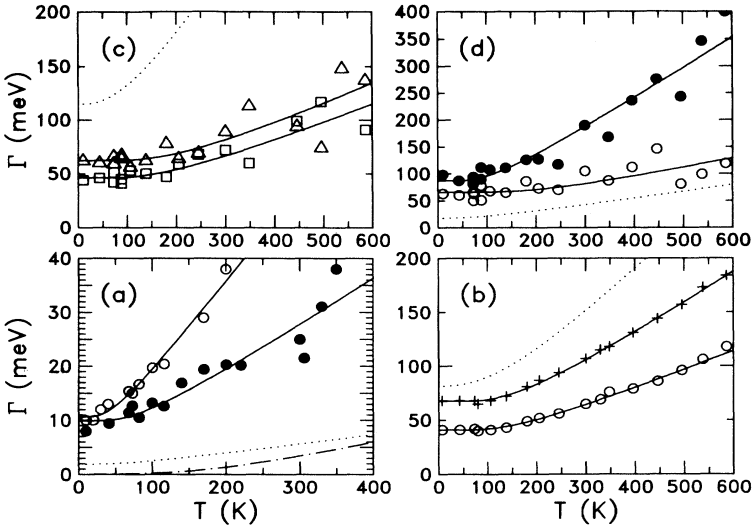

FIG. 9. Broadening parameters Γ of critical points, obtained from a line-shape analysis: (a) E_0 (•) and $E_0+\Delta_0$ (○), with 0D CP's. The solid lines show a fit to the data with Eq. (5), the dashed-dotted line the broadenings due to Fröhlich interaction for uncorrelated electron-hole pairs, the dotted line the calculated broadenings due to intervalley-scattering processes in the valence band. (b) Experimental broadenings of the E_1 critical point when fitted with a 2D (○) or excitonic (+) line shape. Measured broadenings of the (c) $E_2(1)$ (□), and $E_2(2)$ (△) and (d), (b) E_0' (•), and $E_0'+\Delta_0'$ (○) critical points when analyzed with 3D line shapes. The solid lines show a fit to the broadenings with Eq. (5), the dotted lines the results of a parameter-free calculation for the deformation potential-type electron-phonon interaction.

that our analysis is more reliable, since we determine our broadenings from $d^2\epsilon/dE^2$ rather than from straight absorption data. Also, it might seem that our $E_0+\Delta_0$ peak in Fig. 6 is somewhat sharper than the shoulder in Fig. 1 of Ref. 49. The broadenings of the E_1 gap of GaP, fitted with 2D (○) or 0D (+) line shapes, can be found in Fig. 9(b). The parameters for a fit of the data with Eq. (5) are given in Table V. The temperature-independent contribution Γ_1 was set to zero, since the release of this constraint does not improve the fit significantly. We note that the parameter Θ is much larger for the E_1 broadenings than for E_0 (see Sec. IV). Figures 9(c) and 9(d) show the broadenings for the E_0' (•), $E_0'+\Delta_0'$ (○), $E_2(1)$ (□), and $E_2(2)$ (△) CP's when fitted with three-dimensional line shapes. The parameters for Eq. (5) are given in Table V.

The amplitudes A and phase angles ϕ of the E_0 (○) and E_1 (•) CP's are given in Fig. 10, those of E_0' (•), $E_0'+\Delta_0'$ (○), $E_2(1)$ (□), and $E_2(2)$ (△) in Fig. 11. We expect ϕ to be 90° for E_1 (two-dimensional saddle point) and 270° for E_0 (three-dimensional minimum M_0), see Ref. 4. (See also Ref. 14 for a more recent discussion of the physical significance of these phase angles.) The observed phase of E_0 is larger than expected due to excitonic effects which decrease with increasing temperature. The phases of the $E_0'+\Delta_0'$, $E_2(1)$, and $E_2(2)$ CP's are

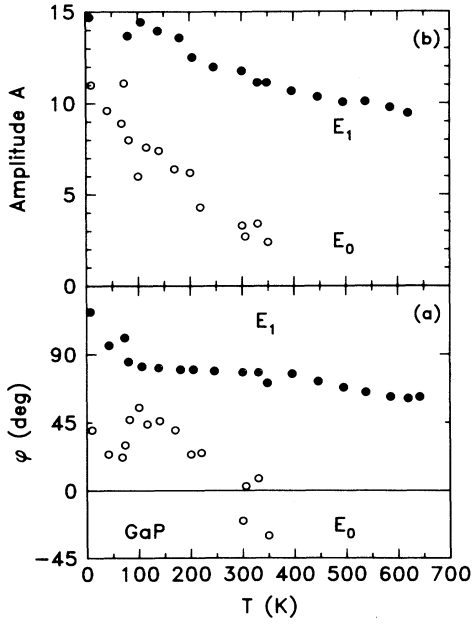

FIG. 10. Amplitudes (b) and phase angles (a) for the E_0 (○) and E_1 (•) CP's, fitted with 3D and 2D line shapes, respectively. The amplitudes are in units of eV^{-1} (1) for a 3D (2D) critical point.

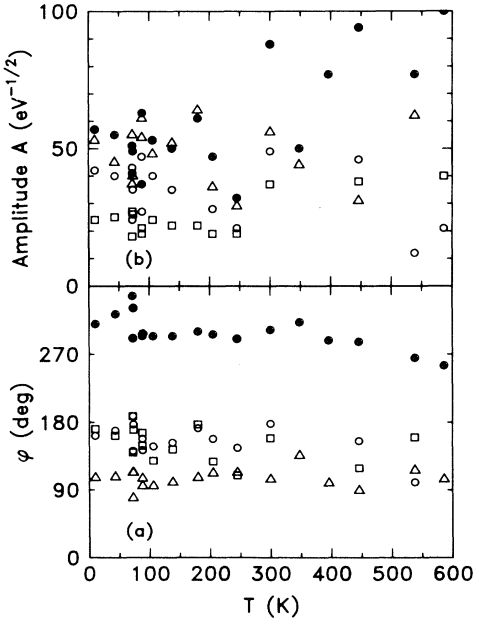

FIG. 11. As Fig. 10, but for the E_0' (•), $E_0'+\Delta_0'$ (○), $E_2(1)$ (□), and $E_2(2)$ (△) CP's (fitted with 3D line shapes).

all between 90° and 180°, whereas that of E_0' is about 270°. Cardona[4] has shown that the amplitude of the E_0 CP is $C_0''/\sqrt{E_0}$, where C_0'' is a universal constant between 1 and 2 related to the momentum matrix element. We thus calculate $A\sim1$, which is several times lower than the observed amplitude. This is also found in other materials[4,28] and attributed to having neglected excitonic effects. The amplitude of the E_1 CP can also be estimated with a simple $\mathbf{k}\cdot\mathbf{p}$ model, see Ref. 101. We obtain A=3 from this model, which is smaller than the observed amplitude also due to excitonic effects, just as in other materials such as GaSb (Ref. 15) or AlSb.[28]

IV. THEORY

A. Pseudopotential band-structure model

The empirical pseudopotential method[81,35] (EPM) has been very useful in the description of semiconductor band structures, see Ref. 35. Usually, the difference between local EPM band-structure data and experimental values is about 0.1 eV close to the gap and up to 1 eV or more for other bands.[81] While this accuracy may be adequate for many purposes, our first attempts to calculate the temperature dependence of CP energies and broadenings failed for GaP and AlSb, especially for the temperature dependence of the lowest indirect gaps. Realizing that this failure could be due to the inadequacy of the 25-year-old form factors of Ref. 81, we decided to find a better set of EPM form factors, as in our earlier work on InP.[102] (An EPM band-structure calculation can only be as good as the experimental data used as input; therefore EPM form factors improve over time with more accurate experimental data.)

We therefore performed a thorough survey of the band-structure literature for GaP and selected a set of energies at Γ, L, and X which seemed to agree best with the most accurate experiments and *ab initio* band-structure calculations.[46] This set of energies (which may well be biased and subject to change with future experiments) is given in Table VI in the column labeled "Input." We then varied the pseudopotential form factors (with the modified Marquardt-Levenberg algorithm using a commercial numerical software package[103]) starting with the values from Ref. 81, until we found the best agreement between the EPM and input energies. In the fitting procedure, a higher weight was given to the better known fundamental band gaps, but even the lowest valence band carried some weight.

The EPM energies thus obtained are given in Table VI in the column labeled "Output." The new set of local EPM form factors is listed in Table VII. We verified that the CB wave functions at the X point have the correct symmetries, i.e., that $E(X_{1c}) < E(X_{3c})$; compare Refs. 104 and 44. We used up to 113 plane waves in the calculations, corresponding to a cutoff of E_1=E_2=16

TABLE VI. Input: Electronic energies (in eV) of GaP at high-symmetry points taken from the literature (Refs. 46, 34, and 54). Output: EPM energies obtained with the new form factors after minimizing the deviation from the input values. The spin-orbit splittings have been removed.

	Input	Output
Γ_{15v}	0.000	0.000
Γ_{1c}	2.877	2.888
L_{1c}	2.664	2.595
X_{1c}	2.377	2.375
X_{3c}	2.717	2.743
L_{3v}	−1.246	−0.999
L_{2v}	−6.8	−6.243
L_{1v}	−10.7	−10.966
L_{3c}	5.55	5.611
Γ_{1v}	−12.0	−12.660
Γ_{15c}	4.87	4.892
X_{5v}	−2.8	−2.364
X_{3v}	−6.8	−6.384
X_{1v}	−9.6	−10.206

TABLE VII. Local empirical pseudopotential form factors (in Rydbergs) obtained by fitting to the "Input" energies of Table VI (New). Values taken from the literature are given for comparison.

Form factor	New	Ref. 81
$V_S(3)$	−0.2428	−0.22
$V_S(8)$	0.0241	0.03
$V_S(11)$	0.0952	0.07
$V_A(3)$	0.0763	0.12
$V_A(4)$	0.0540	0.07
$V_A(11)$	0.0236	0.02
$V_A(12)$	0.0236	0

TABLE VIII. Linear pressure coefficients of CP energies for GaP (in meV/GPa). Where necessary, the experimental bulk modulus of 88 GPa (see Ref. 43) was used to convert deformation potentials to pressure coefficients.

$\frac{dE_i}{dP}$	$\frac{dE_0}{dP}$	$\frac{dE_1}{dP}$	$\frac{dE_0'}{dP}$	$\frac{dE_2}{dP}$	Source
		Experiment			
−11. (1)	107 (10)	58 (6)			Ref. 67
	97 (8)				Ref. 109
−13					Ref. 52
		Theory			
−21.8	95.6				Ref. 43
−24	81	40			Ref. 109
−8	92	46		32	Ref. 110
−26	89	52		16	Ref. 44
−18	100				Ref. 111
−18	117	48		64	Ref. 83
	111				Ref. 112
	106				Ref. 113
−17	86	35		21	Ref. 114
			10[a]		
+30	114	80	38	57	This work

[a]We found no value for this quantity in the literature. We therefore assume that it is ten times smaller than the pressure shift for E_0.

(see Ref. 81) or about 5 Ry. The form factors $V(11)$ and $V(12)$ were set equal to each other. This guarantees that we should be able to find a smooth potential $V(|\mathbf{q}|)$ to interpolate the EPM form factors. With a very simple model for the pressure dependence of the band structure (neglecting the pressure dependence of the dielectric function[83]), we even obtain reasonable pressure coefficients for most gaps, see Table VIII.

B. Temperature dependence of CP energies

The temperature dependence of the CP energies is due to thermal expansion and two electron-phonon contributions, the Debye-Waller (DW) and self-energy (SE) terms, as explained in detail in Refs. 16, 24, and 15. While we do not intend to fully outline the theory of the temperature shifts and its historical development, we mention briefly that the DW term can be calculated fairly easily by multiplying the form factors used in an EPM calculation with the same lattice-dynamical DW factors used in x-ray scattering.[105] Evaluating the SE term is more involved, since a detailed understanding of the deformation-potential interaction is necessary. Baumann[106] estimated this contribution to the shifts of the E_0 gap of GaP using deformation potentials taken from high-field transport measurements.

In this work, we use the formalism described previously,[16,24] which is based on an EPM electronic structure, a shell model for the lattice vibrations,[107,108] and perturbation theory taking into account terms up to second order in phonon displacement. The DW and SE contributions of the phonons with energy Ω to the temperature shifts of an electronic state $n\mathbf{k}$ in band n with wave vector $\mathbf{k}$ are given by

$$(\Delta E_{n\mathbf{k}})_\alpha(T) = \int_0^\infty d\Omega\; g^2 F_\alpha(\mathbf{k}, n, \Omega)(N_\Omega + \tfrac{1}{2}), \quad (6)$$

where N_Ω is the Bose-Einstein factor and α stands for DW or SE. The temperature-independent electron-phonon spectral functions g^2F are shown for various conduction- and valence-band electronic states in Fig. 12. In order to obtain the total change for a given gap, the self-energy and Debye-Waller terms have to be added, and the valence-band shift has to be subtracted from the conduction-band shift. (Absolute shifts of a given state are meaningless in our EPM framework.) In order to obtain the shifts for the E_1 critical point, the results for four points along the ΓL direction were averaged. The point P=(0.75,0.25,0.25) (in units of $2\pi/a$) is representative for the E_2 critical point, the shifts of the E_0' CP were calculated at the Γ point.

The thermal expansion term was calculated using the pressure dependence of the gaps[109–114] in Table VIII and the experimental data for the thermal expansion of GaP.[46,115–117] The results of our calculation (including all three terms) are shown by the dotted lines in Figs. 7 and 8. The curves were shifted vertically to reproduce the measured low-temperature gaps. The agreement is reasonable, in particular when taking into account that our theory does not contain any parameters for the electron-phonon interaction.

C. Broadenings of critical points

Using a similar formalism, with a spectral function g^2B corresponding to the imaginary part of the self-energy term, the broadening parameters Γ of an electronic state $n\mathbf{k}$ can be calculated:

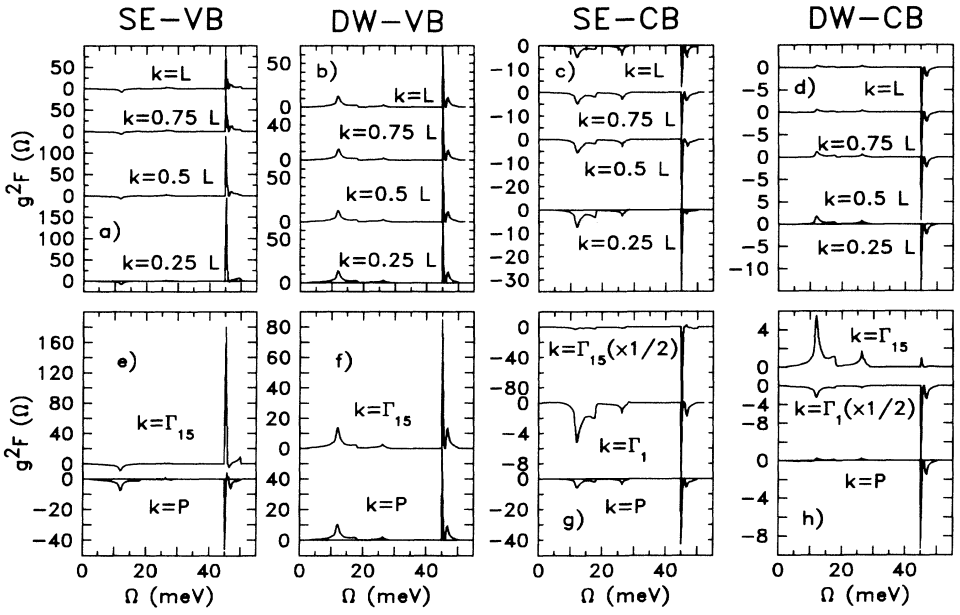

FIG. 12. Electron-phonon spectral functions g^2F as a function of phonon energy Ω for the Debye-Waller (DW) and self-energy (SE) contributions to various conduction- (CB) and valence-band (VB) electronic states.

$$\Gamma_{n\mathbf{k}}(T) = \int_0^\infty d\Omega\ g^2 B(\mathbf{k}, n, \Omega)(N_\Omega + \tfrac{1}{2}). \qquad (7)$$

There are no contributions from the Debye-Waller term or from thermal expansion, but other sources of broadenings, such as instrumental resolution (which is smaller than 5 meV in all of our measurements) or imperfections of the sample (for example, residual surface strain due to polishing) have to be considered. The contributions of the Fröhlich interaction to these broadenings, which are usually small, have to be considered at the Γ point, where the broadenings due to the deformation-potential interaction are also small. The experimentally observed broadening of a gap is the sum of the broadenings of the initial and final states in the valence and conduction bands, respectively.

Figure 9(a) shows the measured broadenings of the E_0 (•) and $E_0 + \Delta_0$ (○) gaps. The deformation-potential interaction causes no broadening of the Γ_8^v valence band, because no final states at the same energies are available for scattering. Intervalence-band scattering (IVBS) from the split-off hole Γ_7^v to the heavy- and light-hole bands, on the other hand, should lead to a nonzero broadening. Therefore, one would expect $\Gamma(E_0+\Delta_0)$ to be larger than $\Gamma(E_0)$. This was observed by Sell and Lawaetz,[49] but not by us. Our results can be explained as follows.

Braunstein and Kane[118] have shown that *optical* intervalence-band transitions between the Γ_7^v (split-off hole) and Γ_8^v (heavy and light hole) bands are forbidden by symmetry. (This can also be seen by direct evaluation of the optical dipole matrix elements using the wave functions given on p. 69, Ref. 4.) The same argument holds for phonon-assisted IVBS processes from Γ_7^v to Γ_8^v, since the operator grad $V_\alpha(r)$ required to calculate the IVBS transition strengths[26] has odd parity, just like the dipole operator. Therefore, the matrix element $\langle \mathbf{q}, n\,|H_{\text{el-ph}}|\,\Gamma_7^v\rangle$ for phonon-assisted IVBS leading to a broadening of the Γ_7^v valence-band state is at least linear in the magnitude q of the phonon. Based on this information, we conclude that for GaP with its very small spin-orbit splitting (Δ_0=0.08 eV) q will be very small and therefore IVBS very weak, much weaker than in other materials such as Ge or GaAs. Therefore, our experimental broadenings are reasonable.

Since the small spin-orbit interactions in GaP were not included in our calculations, we should obtain an average value between the E_0 and $E_0 + \Delta_0$ broadenings (dotted line in Fig. 9). The dashed-dotted line shows an estimate for the contribution of the Fröhlich interaction to the E_0 broadenings, calculated for uncorrelated electron-hole pairs. (Excitonic effects could enhance this contribution, see Ref. 119.) The VB maximum Γ_8^v is only broadened by the Fröhlich interaction (which is small at low temperatures), whereas the conduction-band state Γ_1^c is affected by intervalley scattering processes to the minima at X_1^c, X_3^c, and L_1^c (dotted line). Even with our improved pseudopotentials, the sum of deformation-potential and Fröhlich interaction contributions is much smaller than the observed broadenings. This is somewhat disappointing and could be due to a number of factors: (i) The sample surface is imperfect, (ii) the pseudopotential form factors still do not describe the conduction-band structure accurately, (iii) the analytical line shapes of Eq. (1) (assumed to be excitonic for the E_0 gap) are not adequate for some reason, for example, due to surface electric fields.

The calculated broadenings for the E_1, $E_2(P)$, and E_0' critical points are shown in Figs. 9(b), 9(c), and 9(d), respectively. With our improved pseudopotential form factors, the calculated E_1 broadenings are somewhat larger than reported previously.[18] The agreement between theory and experiment is worse than for the temperature shifts, especially for the E_0' and E_2 critical points. This may result from the fact that the experimental determination of the broadening parameters is very difficult, since they depend on the analytical line shape and other details of the fitting procedure. It would be useful to determine some of these lifetimes directly in the time domain with an optical dephasing experiment. This has recently become possible with the availability of tunable femtosecond pulses in the blue and near-UV spectral regions generated by a frequency-multiplied titanium-sapphire laser system.

V. CONCLUSION

From the dielectric function of GaP at various temperatures between 10 and 640 K, we have obtained the critical-point parameters as a function of temperature. We have shown that the temperature dependence of the various energy gaps can be calculated with reasonable accuracy from a microscopic model, based on empirical pseudopotentials and phonon shell models. The calculated shifts depend somewhat on the particular choice of pseudopotential form factors (and also the choice of the phonon model), but more accurate results can be obtained by adjusting the form factors on the basis of more recent band-structure data.

ACKNOWLEDGMENTS

We would like to thank H. Hirt, P. Wurster, and M. Siemers for expert technical help, A. Böhringer for the pretreatment of the samples, and A. Keckes and E. Schönherr for providing the vapor-phase-epitaxy-grown crystal. The bulk GaP samples were obtained from S. Leibenzeder (Siemens AG, Erlangen, Germany). We are also indebted to U. Schmid for a critical reading of the manuscript. Part of this work was performed at the Ames Laboratory, which is operated for the U.S. Department of Energy by Iowa State University under Contract No. W-7405-Eng-82. The work at Ames was supported by the Director for Energy Research, Office of Basic Energy Sciences.

* Present address: Ames Laboratory and Department of Physics and Astronomy, Iowa State University, Ames, IA 50011-3160. Electronic address: zollner@ALISUVAX or zollner@vaxld.ameslab.gov
† Present address: Centro Nacional de Microelectrónica, Consejo Superior de Investigaciones Científicas, Serrano, 144, E-28006 Madrid, Spain.
‡ Present address: Department of Physics, University of California, Berkeley, Berkeley, CA 94720.
§ Permanent address: Department of Solid State Physics, Faculty of Science, Masaryk University, Kotlářská 2, 611 37 Brno, Czech Republic.
** Present address: Fritz-Haber-Institut der Max-Planck-Gesellschaft, Faradayweg 4-6, D-14195 Berlin (Dahlem), Germany.

[1] D. E. Aspnes and A. A. Studna, Phys. Rev. B **27**, 985 (1983).
[2] L. Van Hove, Phys. Rev. **89**, 1189 (1953).
[3] D. E. Aspnes, in *Handbook on Semiconductors*, edited by M. Balkanski (North-Holland, Amsterdam, 1980), Vol. 2, p. 109; Surf. Sci. **37**, 418 (1973).
[4] M. Cardona, *Modulation Spectroscopy* (Academic, New York, 1969); in *Atomic Structure and Properties of Solids*, edited by E. Burstein (Academic, New York, 1972), p. 514.
[5] B. O. Seraphin, in *Semiconductors and Semimetals*, edited by R. K. Willardson and A. C. Beer (Academic, New York, 1972), Vol. 9, p. 1.
[6] A. Savitzky and M. J. E. Golay, Anal. Chem. **36**, 1627 (1964); corrections in J. Steinier, Y. Termonia, and J. Deltour, *ibid.* **44**, 1906 (1972).
[7] J. W. Garland, C. Kim, H. Abad, and P. M. Raccah, Phys. Rev. B **41**, 7602 (1990).
[8] C. S. Wang and B. M. Klein, Phys. Rev. B **24**, 3393 (1981); **24**, 3417 (1981).
[9] M. Alouani, L. Brey, and N. E. Christensen, Phys. Rev. B **37**, 1167 (1988).
[10] A.-B. Chen, S. Phokachaipatana, and A. Sher, Phys. Rev. B **28**, 1121 (1983).
[11] G. Jungk, Phys. Status Solidi B **105**, 551 (1981).
[12] N. Meskini, H. J. Mattausch, and W. Hanke, Solid State Commun. **48**, 807 (1983).
[13] J. W. Garland, H. Abad, M. Viccaro, and P. M. Raccah, Appl. Phys. Lett. **52**, 1176 (1988).
[14] C. K. Kim, J. W. Garland, H. Abad, and P. M. Raccah, Phys. Rev. B **45**, 11 749 (1992).
[15] S. Zollner, M. Garriga, J. Humlíček, S. Gopalan, and M. Cardona, Phys. Rev. B **43**, 4349 (1991). The broadenings of the E_1 and $E_1 + \Delta_1$ CP's in Table I of this reference (as well as the error bars) should be divided by ten.
[16] M. Cardona and S. Gopalan, in *Progress on Electron Properties of Solids*, edited by R. Girlanda (Kluwer Academic, Deventer, Holland, 1989), p. 51.
[17] S. Zollner, S. Gopalan, and M. Cardona, Solid State Commun. **77**, 485 (1991).
[18] S. Zollner, S. Gopalan, M. Garriga, J. Humlíček, L. Viña, and M. Cardona, Appl. Phys. Lett. **57**, 2838 (1990).
[19] E. Antončik, Czech. J. Phys. **5**, 449 (1955).
[20] J. Camassel and D. Auvergne, Phys. Rev. B **12**, 3258 (1975).
[21] H. Y. Fan, Phys. Rev. **82**, 900 (1951).
[22] P. B. Allen and M. Cardona, Phys. Rev. B **23**, 1495 (1981); **24**, 7479(E) (1981); **27**, 4760 (1983); P. B. Allen and V. Heine, J. Phys. C **9**, 2305 (1976).
[23] P. Lautenschlager, P. B. Allen, and M. Cardona, Phys. Rev. B **31**, 2163 (1985); **33**, 5501 (1986).
[24] C. K. Kim, P. Lautenschlager, and M. Cardona, Solid State Commun. **59**, 797 (1986); S. Gopalan, P. Lautenschlager, and M. Cardona, Phys. Rev. B **35**, 5577 (1987).
[25] S. Zollner, S. Gopalan, M. Garriga, J. Humlíček, and M. Cardona, in *19th International Conference on the Physics of Semiconductors*, edited by W. Zawadzki (Institute of Physics, Polish Academy of Sciences, Warsaw, 1988), p. 1513.
[26] S. Zollner, S. Gopalan, and M. Cardona, J. Appl. Phys. **68**, 1682 (1990); Appl. Phys. Lett. **54**, 614 (1989); Semicond. Sci. Technol. **7**, B137 (1992).
[27] A. Keckes, H. Binder, G. Hofmann, A. Koukitu, and E. Schönherr, Cryst. Prop. Prep. **32-34**, 520 (1991).
[28] S. Zollner, C. Lin, E. Schönherr, A. Böhringer, and M. Cardona, J. Appl. Phys. **66**, 383 (1989).
[29] R. M. A. Azzam and N. M. Bashara, *Ellipsometry and Polarized Light* (North-Holland, Amsterdam, 1977).
[30] D. E. Aspnes, B. Schwartz, A. A. Studna, L. Derick, and L. A. Koszi, J. Appl. Phys. **48**, 3510 (1977).
[31] D. E. Aspnes and A. A. Studna, Rev. Sci. Instrum. **49**, 291 (1978).
[32] L. Viña, S. Logothetidis, and M. Cardona, Phys. Rev. B **30**, 1979 (1984).
[33] M. Cardona, K. L. Shaklee, and F. H. Pollak, Phys. Rev. **154**, 696 (1967).
[34] D. E. Aspnes and C. G. Olson, Phys. Rev. Lett. **33**, 1605 (1974); D. E. Aspnes, C. G. Olson, and D. W. Lynch, Phys. Rev. B **12**, 2527 (1975).
[35] J. R. Chelikowsky and M. L. Cohen, Phys. Rev. B **14**, 556 (1976). See also M. L. Cohen and J. R. Chelikowsky, *Electronic Structure and Optical Properties of Semiconductors* (Springer, Berlin, 1988).
[36] F. Solal, G. Jezequel, F. Houzay, A. Barski, and R. Pinchaux, Solid State Commun. **52**, 37 (1984).
[37] G. P. Williams, F. Cerrina, G. J. Lapeyre, J. R. Anderson, R. J. Smith, and J. Hermanson, Phys. Rev. B **34**, 5548 (1986).
[38] F. H. Pollak, C. W. Higginbotham, and M. Cardona, in Proceedings of the International Conference on the Physics of Semiconductors, Kyoto, 1966 [J. Phys. Soc. Jpn. (Supplement) **21**, 20 (1966)].
[39] A.-B. Chen and A. Sher, Phys. Rev. B **22**, 3886 (1980).
[40] V. A. Singh and A. Zunger, Phys. Rev. B **31**, 3729 (1985); D. M. Wood, A. Zunger, and R. de Groot, *ibid.* **31**, 2570 (1985).
[41] M. Scheffler, J. Bernholc, N. O. Lipari, and S. T. Pantelides, Phys. Rev. B **29**, 3269 (1984).
[42] C. O. Rodríguez, Solid State Commun. **46**, 11 (1983).
[43] P. E. Van Camp, V. E. Van Doren, and J. T. Devreese, Phys. Rev. B **38**, 9906 (1988).
[44] M. Cardona and N. E. Christensen, Phys. Rev. B **35**, 6182 (1987); R. M. Wentzcovitch, M. Cardona, M. L. Cohen, and N. E. Christensen, Solid State Commun. **67**, 927 (1988).
[45] G. B. Bachelet, H. S. Greenside, G. A. Baraff, and M. Schlüter, Phys. Rev. B **24**, 4745 (1981).
[46] O. Madelung, in *Landolt-Börnstein. Numerical Data and Functional Relationships in Science and Technology*, edited by O. Madelung (Springer, Berlin, 1987), Vol. 22a, p. 72. See also Vol. 17a, p. 185 and Vol. 23, p. 43.
[47] S. A. Abagyan, S. M. Gorodetskii, T. B. Zhukova, A. I. Zaslavskii, A. V. Lishina, and V. K. Subashiev, Fiz. Tverd. Tela (Leningrad) **7**, 200 (1965) [Sov. Phys. Solid State **7**,

153 (1965)]; V. K. Subashiev and G. A. Chalikyan, Phys. Status Solidi **13**, K91 (1966).
[48] P. J. Dean, G. Kaminsky, and R. B. Zetterstrom, J. Appl. Phys. **38**, 3551 (1967).
[49] D. D. Sell and P. Lawaetz, Phys. Rev. Lett. **26**, 311 (1971).
[50] M. B. Panish and H. C. Casey, J. Appl. Phys. **40**, 163 (1969); M. R. Lorenz, G. D. Pettit, and R. C. Taylor, Phys. Rev. **171**, 876 (1968); P. J. Dean and D. G. Thomas, *ibid.* **150**, 690 (1966).
[51] S. D. Lacey, Solid State Commun. **8**, 1115 (1970).
[52] A. R. Goñi, K. Syassen, K. Strössner, and M. Cardona, Phys. Rev. B **39**, 3178 (1989).
[53] E. Goldys, P. Galtier, G. Martinez, and I. Gorczyca, Phys. Rev. B **36**, 9662 (1987).
[54] T. Endo, K. Sawa, Y. Hirosaki, S. Taniguchi, and K. Sugiyama, Jpn. J. Appl. Phys. **26**, 912 (1987).
[55] W. G. Spitzer, M. Gershenzon, C. J. Frosch, and D. F. Gibbs, J. Phys. Chem. Solids **11**, 339 (1959).
[56] J. D. Wiley and M. DiDomenico, Phys. Rev. B **1**, 1655 (1970).
[57] A. Onton, Phys. Rev. B **4**, 4449 (1971).
[58] A. N. Pikhtin and D. A. Yaskov, Phys. Status Solidi **34**, 815 (1969).
[59] G. A. Chalikyan, V. K. Subashiev, and P. Kishan, Fiz. Tverd. Tela (Leningrad) **10**, 442 (1968) [Sov. Phys. Solid State **10**, 348 (1968)]; V. K. Subashiev and G. A. Chalikyan, *Ninth International Conference on the Physics of Semiconductors, Moscow* (Nauka, Leningrad, 1968), Vol. 1, p. 375; Phys. Status Solidi **13**, K90 (1966).
[60] D. S. Kyser and V. Rehn, Phys. Rev. Lett. **40**, 1038 (1978).
[61] W. E. Spicer and R. C. Eden, in *Ninth International Conference on the Physics of Semiconductors, Moscow* (Ref. 59), Vol. 1, p. 65.
[62] D. F. Nelson, L. F. Johnson, and M. Gershenzon, Phys. Rev. **135**, A1399 (1964).
[63] T. Nishino, M. Takeda, and Y. Hamakawa, Surf. Sci. **37**, 404 (1973).
[64] M. Cardona, J. Appl. Phys. **32**, 2151 (1961).
[65] H. Ehrenreich, H. R. Philipp, and J. C. Phillips, Phys. Rev. Lett. **8**, 59 (1962).
[66] R. Zallen and W. Paul, Phys. Rev. **134**, A1628 (1964).
[67] R. Zallen and W. Paul, Phys. Rev. **155**, 703 (1967).
[68] M. L. Belle, Zh. I. Alferov, V. S. Grigoréva, L. V. Kradinova, and V. D. Prochukhan, Fiz. Tverd. Tela (Leningrad) **8**, 2623 (1967) [Sov. Phys. Solid State **8**, 2098 (1967)].
[69] A. N. Pikhtin and D. A. Yas'kov, Fiz. Tverd. Tela (Leningrad) **9**, 145 (1967) [Sov. Phys. Solid State **9**, 107 (1967)].
[70] S. S. Vishnubhatla and J. C. Woolley, Can. J. Phys. **46**, 1769 (1968).
[71] J. C. Woolley, A. G. Thompson, and M. Rubenstein, Phys. Rev. Lett. **15**, 670 (1965).
[72] S. E. Stokowski and D. D. Sell, Phys. Rev. B **5**, 1636 (1972).
[73] S. O. Sari and S. E. Schnatterly, Surf. Sci. **37**, 328 (1973).
[74] E. Matagui, A. G. Thompson, and M. Cardona, Phys. Rev. **176**, 950 (1968).
[75] G. Guizetti, L. Nosenzo, E. Reguzzoni, and G. Samoggia, Phys. Rev. B **9**, 640 (1974); L. Nosenzo, E. Reguzzoni, and G. Samoggia, *Eleventh International Conference on the Physics of Semiconductors* (Elsevier, Amsterdam, 1972), p. 1109.
[76] A. G. Thompson, M. Cardona, and K. L. Shaklee, Phys. Rev. **146**, 601 (1966).
[77] C. Alibert, G. Bordure, and A. Laugier, Surf. Sci. **37**, 623 (1973).
[78] T. Takizawa, H. Fukutani, and G. Kuwabara, J. Phys. Soc. Jpn. **35**, 543 (1973).
[79] M. Welkowsky and R. Braunstein, Phys. Rev. B **5**, 497 (1972); R. Braunstein and M. Welkowsky, in *Proceedings of the Tenth International Conference on the Physics of Semiconductors*, edited by S. P. Keller, J. C. Hensel, and F. Stern (U.S. Atomic Energy Commission, Oak Ridge, 1970), p. 439.
[80] T. Takizawa, J. Phys. Soc. Jpn. **52**, 1057 (1983).
[81] M. L. Cohen and T. K. Bergstresser, Phys. Rev. **141**, 789 (1966).
[82] C. Varea de Alvarez, J. P. Walter, M. L. Cohen, J. Stokes, and Y. R. Shen, Phys. Rev. B **6**, 1412 (1972); J. P. Walter and M. L. Cohen, Phys. Rev. **183**, 763 (1969).
[83] I. Gorczyca, Phys. Status Solidi B **125**, 229 (1984).
[84] V. A. Chaldyshev and S. N. Grinyaev, Izv. Vyssh. Ucheb. Zaved Fiz. Inst. Tomsk **3**, 38 (1983) [Sov. Phys. J. High Educ. Instit. Tomsk **3**, 243 (1983)].
[85] D. J. Chadi, Phys. Rev. B **16**, 790 (1977).
[86] F. Lukeš and E. Schmidt, in *Report of the International Conference on the Physics of Semiconductors held at Exeter, July, 1962*, edited by A. C. Stickland (Institute of Physics and Physical Society, London, 1962), p. 389.
[87] T. Endo, S. Taniguchi, T. Yamanaka, M. Kamota, and K. Sugiyama, Jpn. J. Appl. Phys. **25**, 920 (1986).
[88] A. N. Pikhtin, V. T. Prokopenko, and A. D. Yas'kov, Fiz. Tekh. Poluprovodn. **10**, 2053 (1976) [Sov. Phys. Semicond. **10**, 1224 (1976)].
[89] K. Strössner, S. Ves, and M. Cardona, Phys. Rev. B **32**, 6614 (1985).
[90] S. Zollner, Ph.D. thesis, Stuttgart University, Germany, 1991, p. 255.
[91] S. Adachi, Phys. Rev. B **35**, 7454 (1987).
[92] P. Lautenschlager, M. Garriga, L. Viña, and M. Cardona, Phys. Rev. B **36**, 4821 (1987).
[93] G. G. Wepfer, T. C. Collins, and R. N. Euwema, Phys. Rev. B **4**, 1296 (1971).
[94] A. Manoogian and A. Leclerc, Phys. Status Solidi B **92**, K23 (1979); Can. J. Phys. **57**, 1766 (1979).
[95] K. P. O'Donnell and X. Chen, Appl. Phys. Lett. **58**, 2924 (1991). The authors argue that the phonon contribution to the thermal shifts of band gaps should be proportional to the phonon occupation factor N. This statement is misleading. Since phonon absorption and emission are both possible (remember that these transitions are virtual and energy does not have to be conserved), the shifts are approximately proportional to $2N + 1$. This reference also claims that the Varshni model gives a rather poor fit for GaP, C, and Si. This is not surprising, since the Varshni model is an approximation valid only for temperatures higher than the Einstein temperature.
[96] A. Manoogian and J. C. Woolley, Can. J. Phys. **62**, 285 (1984).
[97] Y. P. Varshni, Physica **34**, 149 (1967).
[98] S. Zollner, J. Kircher, M. Cardona, and S. Gopalan, Solid-State Electron. **32**, 1585 (1989).
[99] S. Rudin, T. L. Reinecke, and B. Segall, Phys. Rev. B **42**, 11 218 (1990).
[100] C. H. Grein, S. Zollner, and M. Cardona, Phys. Rev. B **44**, 12761 (1991); S. Zollner, C. H. Grein, and M. Cardona, Proc. SPIE **1677**, 75 (1992); S. Logothetidis, M. Cardona,

and C. Trallero-Giner, J. Appl. Phys. **67**, 4133 (1990); S. Logothetidis, M. Cardona, and M. Garriga, Phys. Rev. B **43**, 11 950 (1991); C. Trallero-Giner, A. Cantarero, M. Cardona, and V. I. Gavrilenko, *ibid.* **42**, 11 875 (1990); C. Trallero-Giner, V. I. Gavrilenko, and M. Cardona, *ibid.* **40**, 1238 (1989).

[101] L. Viña and M. Cardona, Phys. Rev. B **29**, 6739 (1984).

[102] S. Zollner, U. Schmid, N. E. Christensen, and M. Cardona, Appl. Phys. Lett. **57**, 2339 (1990); S. Zollner, S. Gopalan, and M. Cardona, Phys. Rev. B **44**, 13 446 (1991).

[103] We used routine E04CHF from the NAG FORTRAN Library, Mark 14. The IMSL routines ZXSSQ or UNSLF can also be used. NAG and IMSL are registered trademarks of Numerical Algorithms Group Inc., Downers Grove, IL, and IMSL Inc., Houston, TX, respectively.

[104] F. Bassani and M. Yoshimine, Phys. Rev. **130**, 20 (1963).

[105] Y. F. Tsong, B. Gong, S. S. Mitra, and J. F. Vetelino, Phys. Rev. B **6**, 2330 (1972).

[106] K. Baumann, Phys. Status Solidi B **63**, K71 (1974).

[107] P. H. Borcherds, K. Kunc, G. F. Alfrey, and R. L. Hall, J. Phys. C **12**, 4699 (1979).

[108] K. Kunc and O. H. Nielsen, Comput. Phys. Commun. **16**, 181 (1979); **17**, 413 (1979).

[109] S. Ves, K. Strössner, C. K. Kim, and M. Cardona, Solid State Commun. **55**, 327 (1985).

[110] D. L. Camphausen, G. A. N. Connell, and W. Paul, Phys. Rev. Lett. **26**, 184 (1971).

[111] C. G. Van de Walle, Phys. Rev. B **39**, 1871 (1989).

[112] C. Priester, G. Allan, and M. Lannoo, Phys. Rev. B **37**, 8519 (1988).

[113] A. Blacha, H. Presting, and M. Cardona, Phys. Status Solidi B **126**, 11 (1984).

[114] Y. F. Tsay, S. S. Mitra, and B. Bendow, Phys. Rev. B **10**, 1476 (1974).

[115] P. Deus, U. Voland, and H. A. Schneider, Phys. Status Solidi A **80**, K29 (1983).

[116] G. A. Slack and S. F. Bartram, J. Appl. Phys. **46**, 89 (1975).

[117] S. I. Novikova, in *Semiconductors and Semimetals*, edited by R. K. Willardson and A. C. Beer (Academic, New York, 1966), Vol. 2, p. 33.

[118] R. Braunstein and E. O. Kane, J. Phys. Chem. Solids **23**, 1423 (1962).

[119] A. Cantarero, C. Trallero-Giner, and M. Cardona, Solid State Commun. **69**, 1183 (1989); Phys. Rev. B **39**, 8388 (1989); **40**, 12 290 (1989); C. Trallero-Giner, A. Cantarero, and M. Cardona, *ibid.* **40**, 4030 (1989).